Supplementary Information for

Intensifying Conformational Dynamics Enables HRP Catalysis in Organic Phase

Yupei Jian, [‡a] Hai Zhou, [‡a] Yilei Han, [*a] Kaiyi Zhu, [a] Minghao Sun, [a] Shuiwei Zhang, [a] Diannan Lu, [a] Guoqiang Jiang, [a] and Zheng Liu [*a]

a Key Lab of Industrial biocatalysis, Ministry of Education, Department of Chemical Engineering, Tsinghua University, Beijing 100084, China

‡ These authors contributed equally.

* Corresponding Author: Yilei Han, Zheng Liu

Email: hanyl@mail.tsinghua.edu.cn, liuzheng@mail.tsinghua.edu.cn

CONTENT

Methods

1. Materials

Horseradish peroxidase (HRP, ≥250U/mg), Pluronic®F-127, Pluronic®F-108, Dess-Martin periodinane (1,1,1-tris(acetyloxy)-1,1-dihydro-1,2-benziodoxol-3-(1H)-one), sodium cyanoborohydride ($NaCNBH_3$, 95 wt%), 2-methylpyridine borane, trinitrobenzene sulfonic acid (TNBS), 2,2'-azino-bis-(3-ethylbenzodihydrothiazoline-6-sulfonic acid) diammonium salt (ABTS), and formaldehyde solution (37% w/w in aqueous solution) were purchased from Sigma Aldrich (St. Louis, MO, USA). Tert-butyl hydroperoxide was purchased from Zesheng Co., Ltd (Anhui, China). Pluronic®F-68, *o*-cresol, 2,6-dimethylphenol, 2,6-dimethoxyphenol, guaiacol, *o*-phenylenediamine, and hydrogen peroxide solution (30% w/w in water) were purchased from Maclin (China). Purpald (4-amino-3-hydrazino-5-mercapto-1,2,4-triazole， 99 wt.%) and sodium periodate (98%) were purchased from Alfa Aesar. Dichloromethane, diethyl ether, and toluene were purchased from Tongguang (Peking, China). Deuterated toluene was purchased from Cambridge Isotope Laboratories, Inc (Tewksbury, MA, USA). Other chemicals were all of analytical grade.

2. Enzyme Preparation and Activity Assay

2.1 Preparation of Pluronic-HRP conjugates. The liquid HRP was firstly dialyzed against phosphate buffer (Na_2HPO_4/NaH_2PO_4, 10 mM, pH 7.0) at 4°C for 3 days to remove impurities. The protein concentration after dialysis was determined using the BCA method[1]. A portion of the enzyme solution was frozen at -80°C for 4 hours and then dried in a freeze dryer under vacuum to obtain HRP enzyme powder for later use. Pluronic was solved in the phosphate buffer (10mM, pH 7.0), and the amount of Pluronic was adjusted to achieve a 1:1 molar ratio of the polymer's aldehyde group to the enzyme's amino group. The enzyme solution was added to the Pluronic solution, with a final enzyme concentration of 2mg/mL. The mixture was stirred at room temperature for 2 hours. Then, 10% (by mass of polymer) sodium cyanoborohydride was dissolved in a small amount of ice water and then added dropwise into the mixture, and the solution was stirred for another 15 hours at room temperature. For methylpyridine borane, add 2.5% (v/v) of a 1 M ethanolic solution of methylpyridine borane to the mixture. The solution was dialyzed against phosphate buffer (10mM, pH 7.0) at 4°C for 24 hours to remove as much excess polymer as possible, frozen at -80°C for 4 hours and then lyophilized to obtain the Pluronic-HRP conjugates. The aldehyde modification rate of Pluronic was determined by the Purpald colorimetric method[2]. The amino content of HRP of was determined by the TNBS colorimetric method[3] to calculate the extent of polymer modifications.

2.2 Preparation of reduced and oxidized HRP samples. The reduced HRP (R-HRP) sample was prepared by adding an appropriate amount of sodium cyanoborohydride to the polymer-free HRP solution, stirring at room temperature for 15 hours, dialysis, freezing, and vacuum drying to finally obtain R-HRP powder.

To obtain the active intermediate species compound I, the enzyme solution was rapidly mixed with a hydrogen peroxide solution of the same molar concentration (tert-butyl hydroperoxide was used for toluene) and immediately scanned with the UV spectrophotometer.

2.3 Modification and determination of the aldehyde of Pluronic. The aldehyde group was introduced into the Pluronic through terminal aldehyde modification to react with the amino group of the enzyme[4]. First, 4 g of polymer was weighed and dissolved in 200 mL of methylene chloride, then 5 times the molar amount of Dess-Martin oxidant relative to the terminal hydroxyl groups of the polymer was added and stirred for 24 hours at room temperature. After removing most of the solvent using a rotary evaporator, a white turbid solution was obtained. Pre-frozen cold ether (approximately -20°C) was then added to form a precipitate. The precipitates were filtered, washed several times with cold ether 3-5 times, and dried in a fume hood. The aldehyde group modification rate was determined using the Purpald colorimetric method[2], as detailed in the referenced protocol.

The aldehyde group modification rate was determined using the Purpald colorimetric method. The test solution was Pluronic polymer solution at 4 mg/mL using 133 μmol/L dilution of formaldehyde as standard. The Purpald solution was prepared at 30 mmol/L using 2 mol/L NaOH solution as the solvent and the sodium periodate solution was prepared at 30 mmol/L using 0.2 mol/L NaOH solution. In a 96-well plate, 0-50 μL of formaldehyde diluent (with a range of concentration gradients) and test solution (also with a range of concentration gradients) were added to 50 μL of water per well. 50 μL of Purpald solution is then added to each well. 15 minutes later, 50 μL of sodium periodate solution was added to each well. The absorbance at 560 nm was measured using a microplate reader (Mettler Toledo). The rate of aldehyde modification of Pluronic was calculated by comparing the absorbance of the test solution to the slope of the concentration gradient and the slope of the formaldehyde dilution:

$$Aldehyde\ Group\ Modification\ Rate\ (\%) = \frac{c(HCHO) \times k(polymer)}{2 \times c(polymer) \times k(HCHO)} \times 100\%$$

2.4 Determination of the free amino groups in HRP and Pluronic-HRPs. The amino content was determined using the TNBS colorimetric method to ascertain the average number of amino groups per molecule of free enzyme and the extent of polymer modifications. The standard solution and the test solution are 0.1 mmol/L glycine solution in boric acid buffer (pH=9.3) and HRP and Pluronic-HRP solutions at an enzyme concentration of 0.16 mg/mL, respectively. A concentration gradient was set by adding 0-200 μL of the standard and test solutions to a 96-well plate and using buffer to bring the volume up to 200 μL. Before measurement, add 1.25% TNBS solution and protection from light for 2 hours. The absorbance at 420 nm was measured using a microplate reader (Mettler-Toledo). The absorbance and slope of the concentration gradient of the test solution were compared to the slope of the glycine standard solution to calculate the number of amino groups in each HRP, Pluronic-HRP molecule, and thus the polymer modification rate.

2.5 Enzyme activity assay in aqueous solution. Enzyme activity in aqueous solutions was measured at room temperature (25°C) across three parallel experiments using a 10 mmol/L phosphate buffer at pH 7.0 as the solvent and ABTS as the indicator. The reaction medium contained 1 μL of HRP solution with a protein concentration of 0.2 mg/mL, 50 μL of 0.3% hydrogen peroxide solution and 900 μL of ABTS solution at a concentration of 0.5 mmol/L. The activity of HRP was calculated as the change in absorbance at 415 nm for the first 30 seconds after mixing.
For o-cresol, guaiacol, 2,6-dimethylphenol, 2,6-dimethoxyphenol and o-phenylenediamine, the reaction medium contained 1 μL of HRP solution with a protein concentration of 0.2 mg/mL, 50 μL of 0.3% hydrogen peroxide solution and 900 μL of substrate solution with a concentration of 1 mmol/L. The change in absorbance at 413, 475, 421, 467, and 475 nm for 30 seconds was used for activity calculation, respectively. The relative enzyme activity was determined using the activity of the free HRP solution as a reference.

2.6 Enzyme activity assay in toluene. All solutions were prepared using toluene as the solvent. Before the reaction, the solvent and substrates were dried with molecular sieves overnight. All measurements were performed at room temperature (25°C). The reaction rate was calculated by measuring the increase in absorbance of the product at the wavelength of the maximum absorption peak with time using a UV-visible absorption spectrometer. For the substrate *o*-phenylenediamine[5], *o*-cresol[6], guaiacol[7], 2,6-dimethylphenol[8], and 2,6-dimethoxyphenol[9], the wavelengths and molar absorption coefficients are 475 nm (21000 M^{-1} cm^{-1}), 413 nm (23700 M^{-1} cm^{-1}), 475 nm (26600 M^{-1} cm^{-1}), 421 nm (13360 M^{-1} cm^{-1}), and 467 nm (49600 M^{-1} cm^{-1}), respectively. For HRP-Pluronic, 100 μL of Pluronic-HRP solution (2.5 mg/mL) and 20 μL of tert-butyl hydroperoxide (5.5 mol/L) were added to 780 μL of the substrate solution (50 mmol/L). The solution was quickly mixed, and then transferred to the cuvette to measure the absorbance at the corresponding wavelength at regular intervals over 30 seconds. For HRP, 2 mg of enzyme and 120 μL of tert-butyl hydroperoxide (5.5 mol/L) were added to 5.28 mL of substrate solution. About 1 mL of sample was taken out every 10 minutes to measure the absorbance. Three replicates were conducted for each assay. No product was detected under the above conditions in the blank experiment without enzymes.

3. Spectral analysis

3.1 Circular dichroism spectroscopy. CD spectra were recorded at room temperature on the Chirascan circular dichroism spectrophotometer (Applied Photophysics Ltd) with a path length of 1mm. HRP and Pluronic-HRP solutions were prepared in phosphate buffer (10 mmol/L, pH 7.0) at a concentration of 0.3 mg/mL. The spectral data were analyzed using the K2D program[10] on Dicroweb server (http://dichroweb.cryst.bbk.ac.uk) to determine the secondary structure components.

3.2 UV-visible spectroscopy. UV-vis spectra were recorded at room temperature using the UV-vis spectrophotometer (Shimadzu UV-2450) with quartz cells having a 10-mm pathlength. Aqueous samples of HRP and Pluronic-HRP were prepared in phosphate buffer (10 mmol/L, pH 7.0) at a concentration of 3 μmol/L. Organic solution samples were prepared in toluene at the same concentration. The baseline was corrected using the corresponding solvent.

3.3 Raman resonance spectroscopy. Raman resonance spectra were obtained at room temperature on the HORIBA-Evolution laser Raman spectrometer. Aqueous samples of HRP and Pluronic-HRP were prepared in phosphate buffer (10 mmol/L, pH 7.0) at a concentration of 20 mg/mL. Organic solution samples were prepared in toluene at the same concentration. The excitation wavelength was set to 532 nm. The laser power at the sample was typically 30 mW. The spectra were recorded in the range of 1200 to 1700 cm^{-1} over a duration of 3 minutes. Absorption spectra (190−820

nm) were measured immediately prior to and following each Raman experiment. No degradation was detected under the conditions used in this study. All Raman spectra were calibrated using benzene (300−1700 cm^{-1}), toluene (300−1700 cm^{-1}), or d(6)-dimethyl sulfoxide (1700−2200 cm^{-1}) as an external frequency standard. The spectral features of toluene have been subtracted from the resonance Raman spectra obtained in these solvents. Attempts to acquire spectra in toluene were unsuccessful due to the dominate of strong solvent signal peaks.

3.4 ^{1}H low-field nuclear magnetic resonance. All relaxation analyses were conducted at 32°C on the bench-top pulsed NMR Analyzer (Niumag Analytical Instrumental Corporation, Suzhou, China) at a 0.5 T magnetic field (21 MHz resonance frequency for ^{1}) with a 90° (p_{90}) radiofrequency pulse calibrated for 2.32 μs and a 180° (p_{180}) radiofrequency pulse calibrated for 5.12 μs. The HRP, Pluronic and Pluronic-HRP powders were placed in a clean glass tube with a diameter of 10 mm, pre-dried on molecular sieves in an oven at 35 °C for 48 hours. Then deuterated toluene was added to pre-equilibrate at 32 °C for several hours. Mass of samples were controlled to make sure the protein concentration was the same. The Magic Sandwich Echo-Carr–Purcell–Meiboom–Gill (MSE-CPMG) pulse sequence was adopted for probing protein and polymer dynamics. MSE decays were recorded with $\tau_{MSE} = 4p_{90} + 7\tau_{\phi}$, where τ_{ϕ} was 2 μs, and for CPMG signal acquisition, 10000 echoes were spaced by a duration of $\tau_{CPMG} = 1$ ms. The signals were analyzed by applying a Laplace inverse transform to a multi-exponential decay, fitting with the SIRT algorithm[11] under 10,000 iterations using Niumag analysis software. The inversion method for all samples was the same.

4. Molecular dynamics simulation

4.1 Systems and parameters. The native HRP structure which contains 306 amino acids (PDB code: 1ATJ) was used. The 404 water molecules in the structure were retained as the enzyme-bound water. Pluronic F68 (PEO76-PPO29-PEO76) was constructed by concatenating the structurally optimized segments using Gaussview. Experimental results showed that each HRP molecule was conjugated with about 1 polymer molecule. According to the p*Ka*[12] and SASA of lysines on the protein surface (**Table S5**) indicated Lys232 was inferred as the most likely conjugated site. The F68-HRP structure was then constructed by connecting the Nz atom of lysine's amino terminus to the C atom of the first segment of F68.

4.2 Simulation. Molecular dynamics simulations were performed using Gromacs 2019.4 software[13]. The long-range electrostatics of the system were calculated using the Particle-Mesh-Ewald (PME) method. The cutoff value for short-range electrostatic interactions was set to 1.0 nm. The van der Waals interaction was calculated using the cutoff method and the cutoff distance was set to 1.0 nm.

For the free HRP system, the simulation temperature was set to 298.15 K. The energy was minimize using the conjugate gradient (cg) method until the force of the system was less than 500 kJ/mol/nm, with a maximum of 2000 iterations. Then, conduct a 100 ps simulation under the NPT ensemble, restricting the protein and its bound water to relax the toluene solvent. A 120 ns production molecular simulation was done under the NPT ensemble, setting the pressure to 1 bar, the step size to 1 fs, and the intervals for saving the simulation trajectory to 10,000 steps. Periodic boundary conditions were applied in the x, y, and z directions.

The F68-HRP conjugate system was constructed and simulated as depicted in **Figure S8**. The four stages for the whole MD simulation are (a) Conjugation: Combine the structure and force field files of polymers and HRPs to construct HRP-polymer complexes. (b) Use the pull code to draw the polymer towards the enzyme, reducing the system's box size. (c) Solvate the system by adding toluene molecules, followed by a 40ns MD to relax the polymer at 600K using the NPT ensemble, while the enzyme and the molecular waters are frozen. (d) Remove all the toluene molecules in the system and re-solvate the system with toluene. Run a 120ns production MD at 298K using the NPT ensemble.

The F68-HRP conjugate system was constructed and simulated as depicted in **Figure S8**. The four stages for the whole MD simulation are (a) Conjugation: Combine the structure and force field files of polymers and HRPs to construct HRP-polymer complexes. (b) Use the pull code to draw the polymer towards the enzyme, reducing the system's box size. (c) Solvate the system by add.

4.3 Modelling of F68-HRP in toluene. Firstly, unfold the manually constructed polymer chain with a pulling code to reduce the system's box size. Here are the detailed parameterizations: the F68-HRP was placed in a vacuum box with the HRP and its bound water molecules freeze. The harmonic constraint was set between the polymer side chains

and other system atoms (pull = umbrella) with a force constant of 4000 kJ mol-1 nm-1. The pulling point was initially at the center of mass of the polymer side chain and moved at 0.15 nm/ps along the line connecting the two centers of mass. The polymer-folded conformation was selected from the MD trajectory after approximately 100 ps of simulation. Next, relax the polymer conformation by adding solvent toluene to the box and conducting a 40 ns molecular simulation. The simulation was done under the NPT ensemble, with constraints on HRP and its bound water molecules. The pressure was set to 1 bar, the temperature to 600 K, and step size to 1 fs. After equilibrium of the protein and water molecule conformation at 600K, re-add the solvent toluene molecules and carry out a 120 ns molecular simulation under the NPT ensemble. The pressure was set to 1 bar, temperature to 298.15 K, and step size to 1 fs. The resulting MD trajectory was used for further analysis.

4.4 Protein conformation analysis. The trajectories were analyzed and visualized using Gromacs 2019.4[13], VMD[14], Pymol[15] and mdtraj (1.9.4)[16]. For HRP in toluene, F68-HRP in toluene, and HRP in water, structural properties were calculated using trajectory frames sampled every 5 ps from the 20-120 ns interval. Principal component analysis (PCA) was performed using the Cartesian coordinates of the protein backbone atoms (N, Cα, C, and O). The variance-covariance matrix was computed and diagonalized to generate eigenvectors, which were projected onto the trajectory to construct the free energy landscape. The root-mean-square fluctuation (RMSF) was calculated using the built-in Gromacs function *gmx rmsf*. The aligned reference frame was taken at 20 ns, and the calculation included only protein atoms, excluding hydrogen atoms and the Pluronic segment. Changes in substrate pocket volume were calculated using POVME 3.0[19].

4.5 Substrate transport property analysis. The final frames of the trajectories were used for substrate channel and transport analysis. The Caver Web[17] and Caver Dock[18] was used to identify the substrate channel and calculate energy barriers, substrate binding rate constants, and dissociation ones. The conformations of substrates, such as, *o*-phenylenediamine, *o*-cresol, guaiacol, 2,6-dimethylphenol, and 2,6-dimethoxyphenol were downloaded from PubChem database and optimized by Gaussian using B3LYP/6-31G** level. In brief, the ligand was continuously docked along the identified tunnel in a static protein structure, and the energy profile associated with transport through the channel was used for kinetic inference. Based on Arrhenius-type relationships, the energy barriers represented by $E_{max} - E_{surface}$ and $E_{max} - E_{bound}$ were used to estimate the substrate binding and dissociation rate constants, respectively[18].

4.6 Conformational feature analysis. The content of secondary structure was calculated using the *compute_dssp* function in mdtraj (1.9.4) with the parameter *simplified = True*. The number of hydrogen bonds was calculated using the built-in Gromacs function *gmx hbond*. Solvent-accessible surface area (SASA) was calculated using the *shrake_rupley* function in mdtraj (1.9.4) with the parameter *mode = 'residue'*.

Supplementary Figures

Figure S1. (A) CD spectroscopy data and (B) secondary structure contents of HRP catalysts in aqueous solution

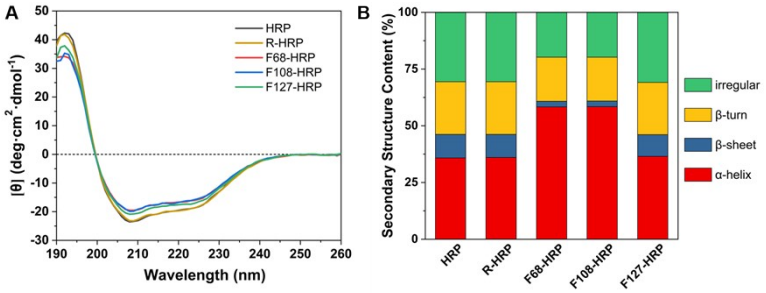

Figure S2. Activity of enzyme catalysts in aqueous solution towards (A) o-phenylenediamine, (B) 2,6-dimethoxyphenol, (C) guaiacol, (D) o-cresol, and (E) 2,6-dimethylphenol in aqueous solution

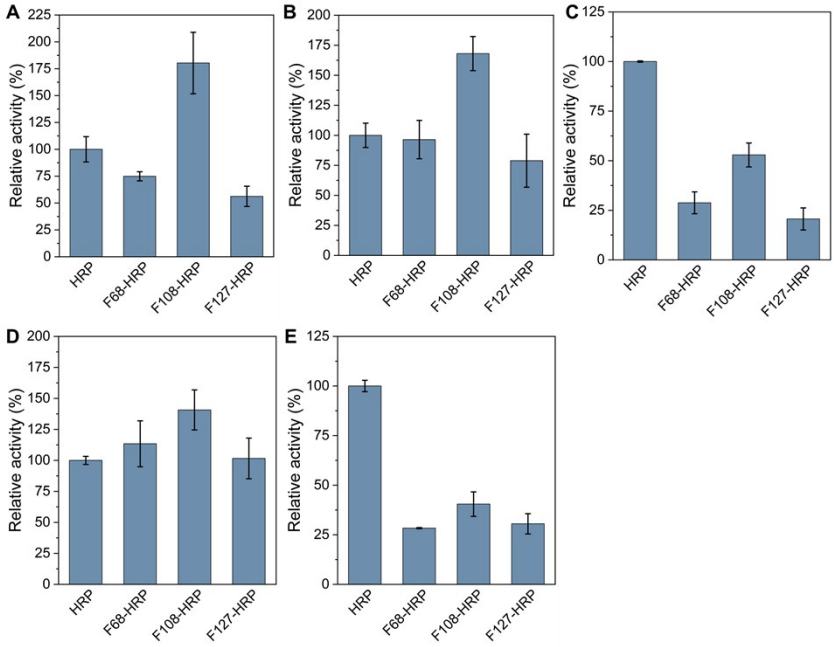

Figure S3. UV-vis absorption spectra of HRP catalysts in aqueous solution for compound I analysis

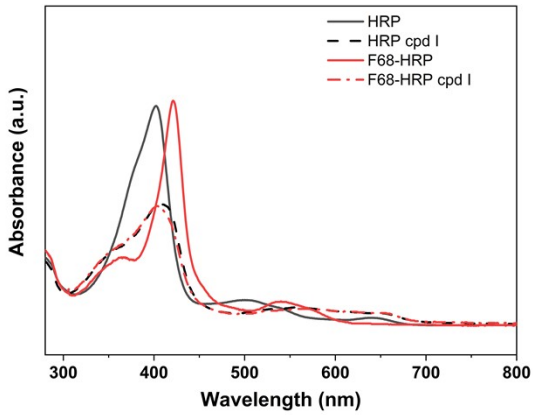

Figure S4. UV-vis absorption spectra and activity of F127-HRP reduced by 2-methylpyridine Borane and sodium cyanoborohydride.

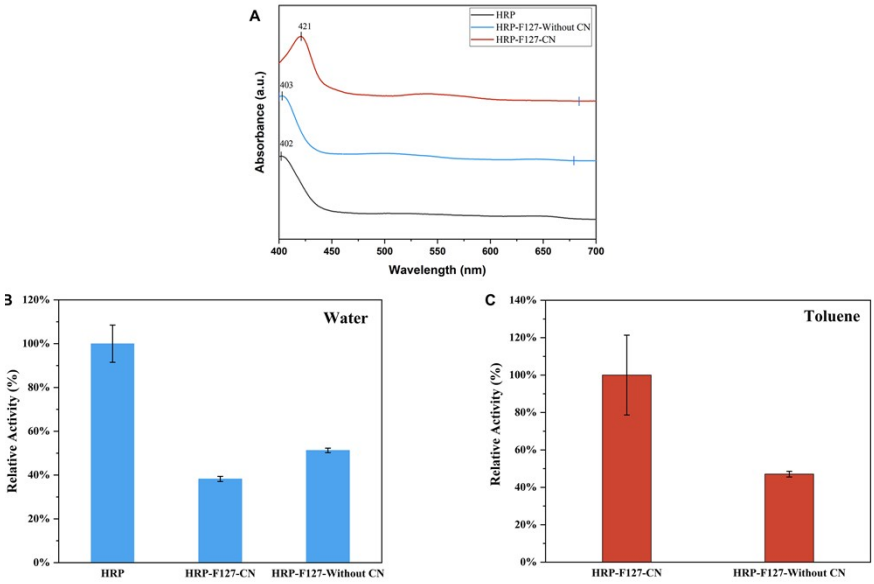

The conjugated enzyme prepared using the non-cyanide reducing agent 2-methylpyridine borane exhibited slightly higher activity in the aqueous phase than that prepared with sodium cyanoborohydride (ABTS was used as the substrate); however, its activity in toluene was only half that of the conjugated enzyme obtained with the cyanide reducing agent (guaiacol was used as the substrate), indicating that the latter affords more effective surface conjugation.

Figure S5. Raman spectra of Pluronics.

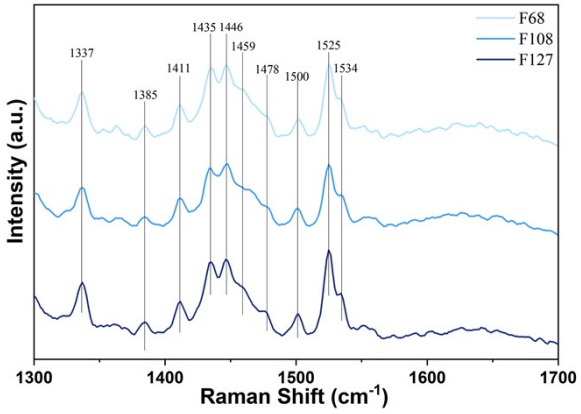

Figure S6. (A) Transverse relaxation time(T_2) of HRP catalysts in toluene; (B) LF-NMR relaxation spectra of HRP in aqueous solution

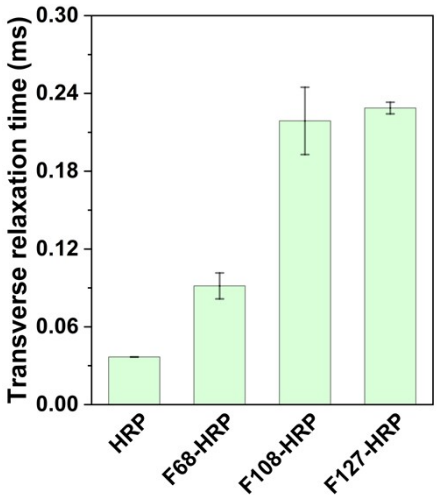

Figure S7. Correlation between transverse relaxation time(T_2) and activity of HRP catalysts in toluene

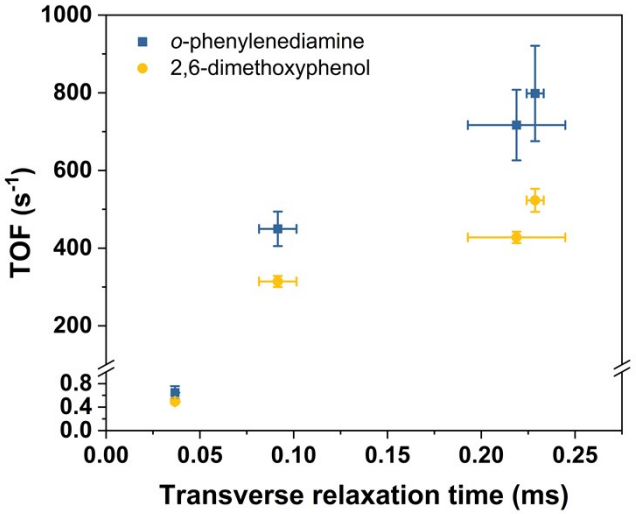

The catalysts, from left to right, are HRP, F68-HRP, F108-HRP, and F127-HRP, respectively.

Figure S8. Molecular simulation procedure. (A) Four stages of modelling and molecular simulation; (B) RMSD of the protein backbone atoms for the F68-HRP over time

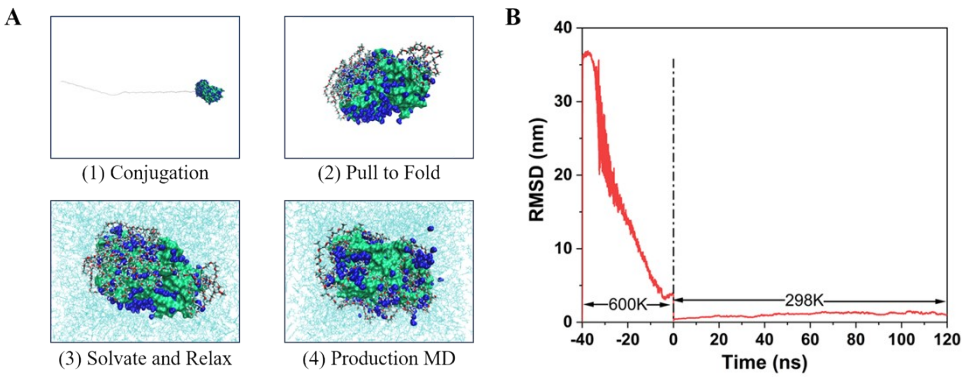

Figure S9. Conformation space and representative conformation for HRP-W, HRP-T and HRP-F68-T.

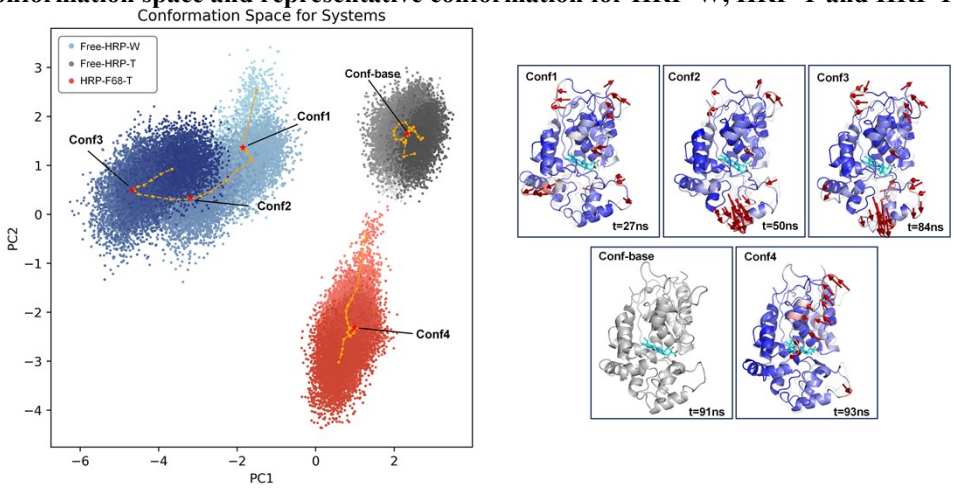

Left panel: A conformational space plot was generated by projecting a 100-ns simulation trajectory, sampled every 5 ps, onto the first two principal components (PC1 and PC2) derived from principal component analysis (PCA) of the Cartesian coordinates of the protein backbone atoms (N, Cα, C, and O). The data points for each system were colored based on their corresponding frames, transitioning from light to dark shades to represent the temporal evolution of the trajectory. A 20-ns sliding window with 5-ns interval was applied to compute the mean conformation within each window, and the resulting points were connected with a yellow dashed line to depict the conformational evolution.

Right panel: Representative conformations were selected along the conformational evolution path near the centroids of conformational clusters:

- HRP-W: Conf1 (t = 27 ns), Conf2 (t = 50 ns), and Conf3 (t = 84 ns)
- HRP-T: Conf-base (t=91 ns)
- HRP-F68-T: Conf4 (t=93 ns)

Using the HRP-T conformation as the reference, deviations of the other conformations relative to it were analyzed. These deviations were visualized with red arrows, where longer arrows indicate larger deviations. The analysis revealed that the loop region of the conjugated enzyme retains substantial flexibility, suggesting enhanced dynamic behavior in this region.

Figure S10. Analysis of distance between crucial residues and SASA of Arg38 in active site for HRP-W, HRP-T and HRP-F68-T.

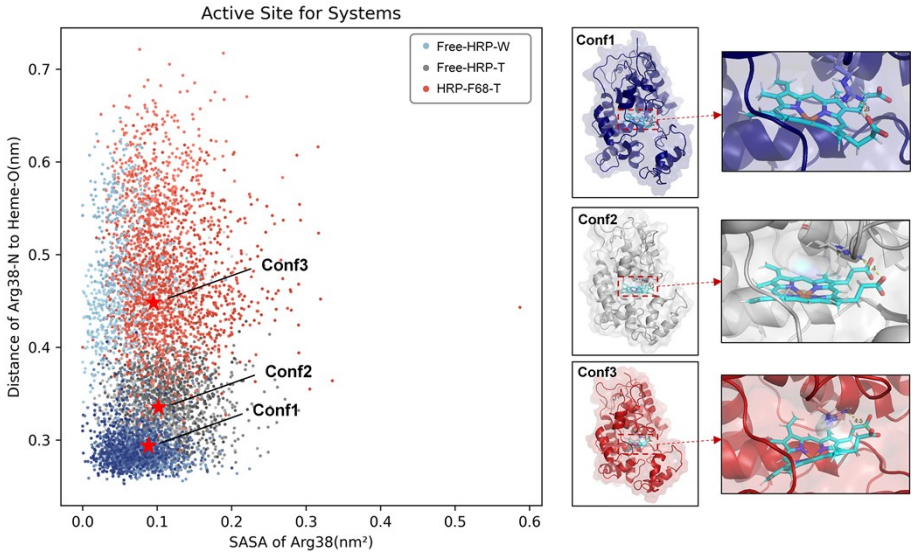

Left panel: The scatter plot displays the solvent-accessible surface area (SASA) of Arg^{38} on the x-axis and the distance between Arg^{38}–NH1 and heme–O1 on the y-axis. Each data point corresponds to a conformation sampled every 50 ps along the simulation trajectory from 20 to 120 ns, resulting in a total of 2000 data points. The data points for each system were colored based on their corresponding frames, transitioning from light to dark shades to represent the temporal evolution of the trajectory.

Right panel: Representative conformations near the cluster centroids of the three systems were selected for analysis: HRP-W: Conf1; HRP-T: Conf2; HRP-F68-T: Conf3, with both the global structures and active-site details shown.

Figure S11. (A) RMSF (Root Mean Square Fluctuation) of HRP in toluene, HRP in water, and F68-HRP in toluene and (B) Structure of HRP

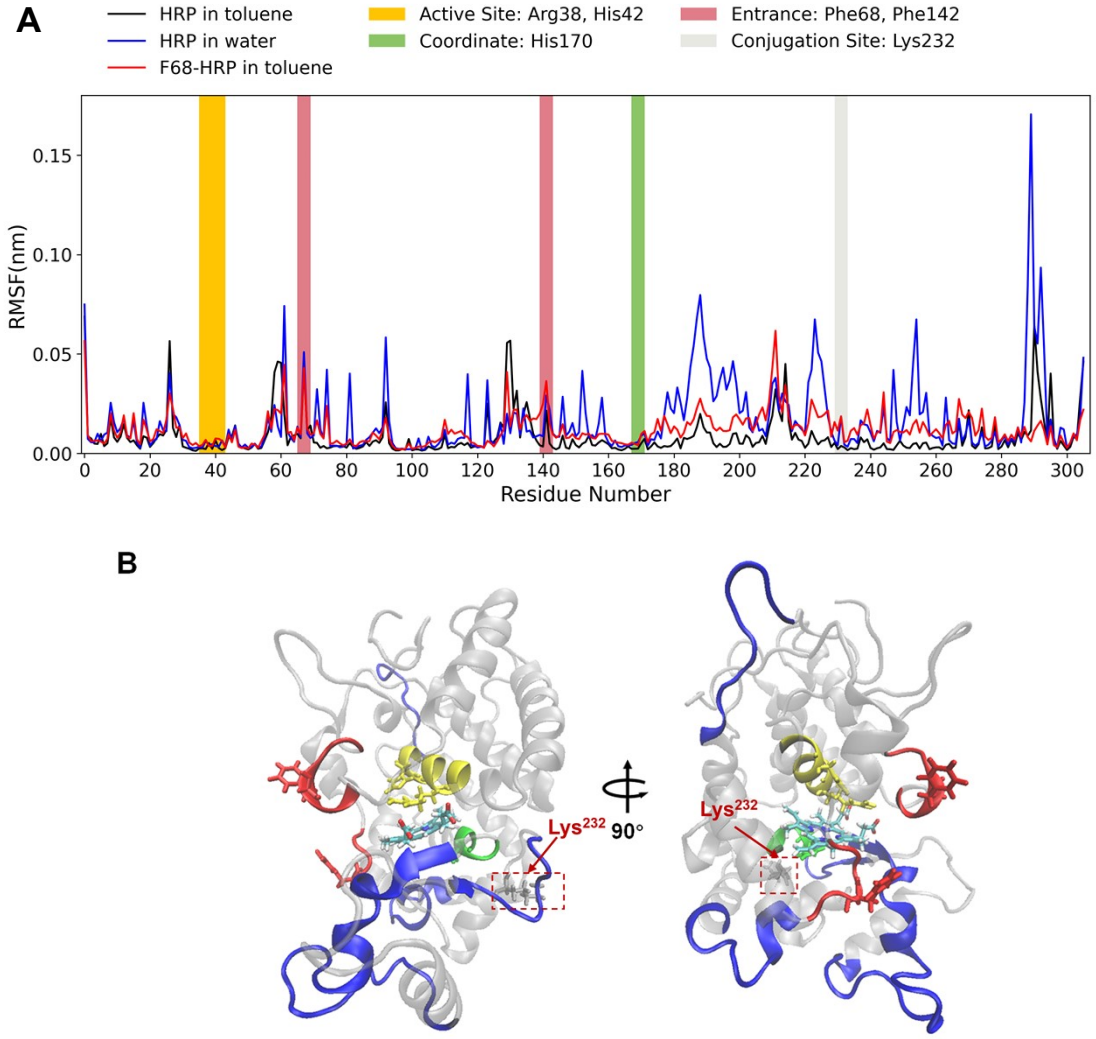

Different colored regions indicate the regions where the functional amino acid residues are located, i.e. the active site (yellow): Arg^{38} and His^{42}, the entrance of the active pocket (red): Phe^{68} and Phe^{142}, the site of coordination with the heme(green): His^{170}, and the site of conjugation with Pluronic(gray): Lys^{232}. The blue region represents the structural domain with higher RMSF in the aqueous phase (resid 175 to 200, 220 to 228, 250 to 260, 287 to 295), which is usually the disordered regions located at the surface of the protein.

Figure S12. Analysis of active pocket for HRP-W, HRP-T and HRP-F68-T.

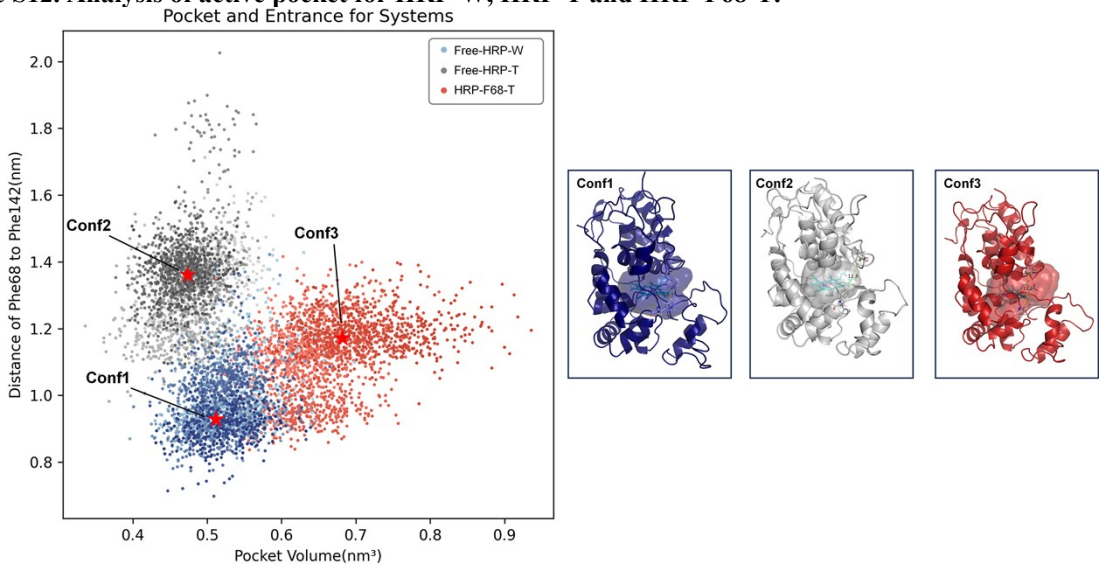

Left panel: Scatter plot with the x-axis showing the active-site pocket volume and the y-axis showing the distance between the centers of mass (COMs) of the Phe^{68} and Phe^{142} side-chain phenyl rings at the pocket entrance. Each data point corresponds to a conformation sampled every 50 ps along the simulation trajectory from 20 to 120 ns, resulting in a total of 2000 data points. The data points for each system were colored based on their corresponding frames, transitioning from light to dark shades to represent the temporal evolution of the trajectory.

Right panel: Representative conformations near the cluster centroids of the three systems were selected for analysis (HRP-W: Conf1; HRP-T: Conf2; HRP-F68-T: Conf3), showing the overall structures, pocket volumes, and inter-residue (Phe^{68}–Phe^{142}) distances.

Figure S13. The transport energy barrier profile of (A) *o*-phenylenediamine, (B) 2,6-dimethoxyphenol, (C) guaiacol, (D) *o*-cresol and (E) 2,6-dimethylphenol for HRP in water, HRP in toluene and F68-HRP in toluene

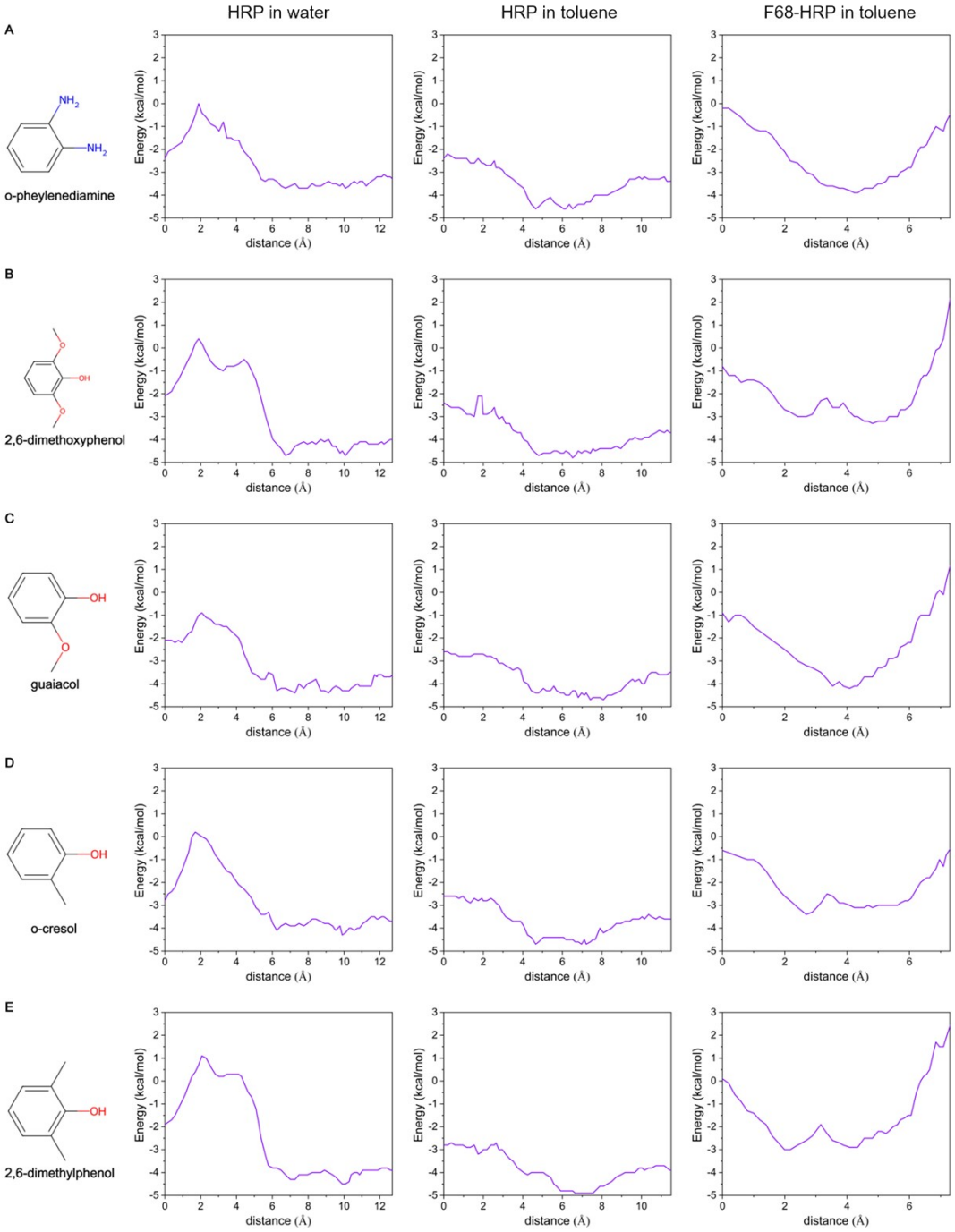

The x-axis represents the distance from the small-molecule substrate to the active site.

Supplementary Tables

Table S1. The property of Pluronics

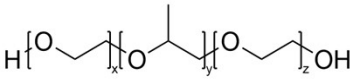

	Molecular formula	Mw (Da)	EO Content (%)	HLB[a]	Aldehyde Group Modification Rate[b] (%)
F68	PEO_{76}–PPO_{29}–PEO_{76}	8400	84.06	29	18.88
F127	PEO_{99}–PPO_{65}–PEO_{99}	12600	75.46	22	23.50
F108	PEO_{132}–PPO_{50}–PEO_{132}	14600	84.06	27	19.67

a. HLB stands for hydrophilic–lipophilic balance

Table S2. The number of free amino groups of HRP and Pluronic-HRPs

Catalyst	The number of amino groups per protein[a]
HRP	3.80
F68-HRP	2.74
F127-HRP	2.80
F108-HRP	3.34

Table S3. Solubility of five substrates in water

Chemical	Solubility in water (mg/L)
o-phenylenediamine	< 1 (20 °C)
2,6-dimethoxyphenol	60.5 (25 °C)
guaiacol	Easily soluble
o-cresol	25.9 (25 °C)
2,6-dimethylphenol	20 (13 °C)

Table S4. Structural properties of HRP and F68-HRP in toluene predicted by MD simulation

Descriptor	Object	HRP in water	HRP in toluene	F68-HRP in toluene
secondary structure (%)[a]	**α-helix**	45.7±1.6	49.2±1.4	48.6±1.4
	β-sheet	3.1±0.7	3.1±0.6	3.4±0.6
	coil	51.2±1.8	48.6±1.4	48.0±1.4
#H-bond[b]	**protein-heme**	8.0±1.4	7.2±0.8	6.8±1.0
	protein-protein	226±7.5	263.1±6.5	261.1±6.9
	protein-water	646±14.2	418.9±10.5	415.1±9.2

a. The content of secondary structure was calculated using the function *compute_dssp* with *simplified = True* in mdtraj (1.9.4).
b. The number of hydrogen bonds were calculated using the built-in Gromacs function *gmx hbond*.

Table S5. The protonation state and SASA for lysines in HRP at pH = 7.0

Residue id	p*Ka*[a]	SASA[b] (nm^2)
65	> 12	0.269
84	> 12	0.028
149	> 12	0.210
174	11.9	0.842
232 (Conjugation Site)	11.2	0.434
241	11.2	0.345

a. The H++ tool (http://newbiophysics.cs.vt.edu/H++/) was used to calculate the p*Ka* for the terminal amino group of lysines in HRP at pH=7.0.
b. A 2 ns molecular simulation was performed for HRP in water to calculate the solvent accessible surface area (SASA) for each lysine. The MD was done with Gromacs, with amber99sb-ildn as the force field, TIP3P as the water model. One water molecule was replaced by Na+ to neutralize the charge.

References

1. O. Classics Lowry, N. Rosebrough, A. Farr and R. Randall, *J biol Chem*, 1951, **193**, 265–275.
2. M. Quesenberry and Y. Lee, *Analytical biochemistry*, 1996, **234**, 50–55.
3. Z. Ding, G. Chen and A. S. Hoffman, *Bioconjugate chemistry*, 1996, **7**, 121–125.
4. J. Zhu, Y. Zhang, D. Lu, R. N. Zare, J. Ge and Z. Liu, *Chemical Communications*, 2013, **49**, 6090–6092.
5. N. Tyagi and P. Mathur, *Spectrochimica Acta Part A: Molecular and Biomolecular Spectroscopy*, 2012, **96**, 759–767.
6. D. P. Provencal, Involvement of free radicals in peroxidatic reactions catalyzed by chloroperoxidase, 1992.
7. L. Setti, S. Scali, I. Degli Angeli and P. G. Pifferi, *Enzyme and Microbial Technology*, 1998, **22**, 656–661.
8. A. Chernykh, N. Myasoedova, M. Kolomytseva, M. Ferraroni, F. Briganti, A. Scozzafava and L. Golovleva, *Journal of applied microbiology*, 2008, **105**, 2065–2075.
9. H. Wariishi, K. Valli and M. H. Gold, *Journal of biological chemistry*, 1992, **267**, 23688–23695.
10. L. Whitmore and B. Wallace, *Nucleic acids research*, 2004, **32**, W668–W673.
11. A. C. Kak and M. Slaney, *Principles of computerized tomographic imaging*, SIAM, 2001.
12. R. Anandakrishnan, B. Aguilar and A. V. Onufriev, *Nucleic acids research*, 2012, **40**, W537–W541.
13. M. J. Abraham, T. Murtola, R. Schulz, S. Páll, J. C. Smith, B. Hess and E. Lindahl, *SoftwareX*, 2015, **1**, 19–25.
14. W. Humphrey, A. Dalke and K. Schulten, *Journal of molecular graphics*, 1996, **14**, 33–38.
15. W. L. DeLano, *CCP4 Newsl. Protein Crystallogr*, 2002, **40**, 82–92.
16. R. T. McGibbon, K. A. Beauchamp, M. P. Harrigan, C. Klein, J. M. Swails, C. X. Hernández, C. R. Schwantes, L.-P. Wang, T. J. Lane and V. S. Pande, *Biophysical journal*, 2015, **109**, 1528–1532.
17. J. Stourac, O. Vavra, P. Kokkonen, J. Filipovic, G. Pinto, J. Brezovsky, J. Damborsky and D. Bednar, *Nucleic acids research*, 2019, **47**, W414–W422.
18. O. Vavra, J. Filipovic, J. Plhak, D. Bednar, S. M. Marques, J. Brezovsky, J. Stourac, L. Matyska and J. Damborsky, *Bioinformatics*, 2019, **35**, 4986–4993.
19. J. D. Durrant, C. A. F. de Oliveira and J. A. McCammon, *Journal of Molecular Graphics and Modelling*, 2011, **29**, 773–776.